Modulation of Atherothrombotic Factors: Novel Strategies for Plaque Stabilization

Bot, I.

2

Serine Protease Inhibitor Serp-1 Strongly Impairs Atherosclerotic Lesion Formation and Induces a Stable Plaque Phenotype in ApoE$^{-/-}$ Mice

Ilze Bot, Jan H. von der Thüsen, Marjo M.P.C. Donners*, Alexandra Lucas[$], Madelon L. Fekkes, Saskia C.A. de Jager, Johan Kuiper, Mat J.A.P. Daemen*, Theo J.C. van Berkel, Sylvia Heeneman*, Erik A.L. Biessen

Division of Biopharmaceutics, Leiden/Amsterdam Center for Drug Research, Leiden University, Leiden, The Netherlands,
*Department of Pathology, Cardiovascular Research Institute Maastricht, University of Maastricht, Maastricht, The Netherlands,
[$]John P. Robarts Research Institute, Vascular Biology Research Group, University of Western Ontario, London, Ontario, Canada.

Circulation Research, 2003, 93: 464-471

Abstract

The myxoma virus protein Serp-1 is a member of the serine protease inhibitor superfamily. Serp-1 potently inhibits human serum proteases including plasmin, uPA and tPA. Serp-1 also displays a high anti-inflammatory activity, rendering it a promising candidate for anti-atherosclerotic therapy. In this study we have thus examined the effect of Serp-1 on *de novo* atherosclerotic plaque formation and on advanced lesions. Perivascular collars were placed around carotid arteries of ApoE$^{-/-}$ mice to induce atherosclerotic plaques and Serp-1 treatment started at week 1 and week 5 after collar placement. Effects of Serp-1 on *de novo* atherogenesis were characterized by a significantly lower plaque size than that of control mice ($18 \pm 5*10^3$ μm^2 versus $57 \pm 12*10^3$ μm^2, resp.; P=0.007). Immunostaining showed a 50% (P=0.004) decrease in the MOMA-2 stained lesion area of Serp-1 treated mice. Treatment of advanced lesions with Serp-1 resulted in a decrease in plaque size and lumen stenosis (P=0.028). α-Actin staining of these lesions was significantly increased compared to the control (P=0.017). In both studies, a higher cellularity of the plaque and increased collagen content was observed in Serp-1 treated mice. *In vitro* studies showed that Serp-1 induces proliferation and migration of vascular smooth muscle cells. In conclusion, Serp-1 inhibits carotid artery plaque growth and progression in ApoE$^{-/-}$ mice. Equally relevant, it enhances cellularity of the plaque core potentially leading to improved plaque stability. The above results indicate that Serp-1 constitutes a promising lead in anti-atherosclerotic therapy.

Introduction

Atherosclerosis is a complex inflammatory disease afflicting medium and large sized arteries. In addition to the cellular constituents of the atherosclerotic plaque, which are primarily of smooth muscle cell, monocytic and lymphocytic origin, a plethora of paracrine and autocrine mediators have been found to be instrumental in atherogenesis[1]. These include components of the coagulation[2,3], fibrinolytic[4] and complement activation[5,6] cascades, which are known to be present in atherosclerotic plaques and to exert a variety of pro-inflammatory effects[7,8]. Moreover, the serine proteases responsible for the generation of factors belonging to these cascades are themselves believed to exert pleiotropic effects, including the upregulation of cytokine responses, receptor activation, extracellular matrix remodelling, as well as cellular migration and proliferation of smooth muscle cells[9,10]. All of these processes have been implicated in the pathogenesis of atherosclerosis and their inhibition could therefore constitute an attractive strategy for the prevention of atherosclerotic plaque formation and/or progression.

A major subgroup of these inhibitors consists of the so-called serpins, which belong to a conserved superfamily of single-chain proteins that act as irreversible covalent 'suicide' protease inhibitors[11]. The precise relevance of these inhibitors to atherosclerosis is largely unclear. Thus, some researchers have found the serpin plasminogen activator inhibitor-1 (PAI-1) to have no effect on *de novo* atherogenesis in hypercholesterolemic mice[12], whereas others have demonstrated PAI-1 deficiency to be atheroprotective in early atherosclerosis[2] and to accelerate plaque progression in advanced atherosclerosis[13]. Its effect in restenosis appears to be more clear-cut, as studies have demonstrated an exacerbating role for PAI-1 in neointima formation by promoting smooth muscle cell migration and proliferation[14-17].

In the quest for an atheroprotective serpin with therapeutic potential, attention has turned to virally-encoded protease inhibitors. The myxoma virus serpin, Serp-1, is a secreted glycoprotein that protects virally infected cells from clearance by the host's immune system by inhibiting the early inflammatory response[18-21]. It has been found to inhibit a range of pro-inflammatory proteases which are considered to be involved in atherogenesis, including urokinase-type plasminogen activator (uPA), tissue-type plasminogen activator (tPA), plasmin and Xa[22,23]. Infusion of Serp-1 protein has been reported to attenuate post-angioplasty plaque formation[24,25] and transplant vasculopathy[25,26,27] in a variety of animal models. Its effect on atherosclerosis remains uncharted, however, as the experience gained with PAI-1 implies that data obtained from endothelial injury experiments cannot necessarily be extrapolated to a beneficial effect in *de novo* atherogenesis.

In this study, we therefore aimed to delineate the effect of Serp-1 on *de novo* carotid atherogenesis and lesion progression in atherosclerosis-prone ApoE knockout ($ApoE^{-/-}$) mice. Accelerated atherosclerotic plaque formation was induced by perivascular collar placement as described previously[28] and Serp-1 glycoprotein was administered one (effect on *de novo* plaque formation) or

five weeks (effect on advanced lesions) after collar placement by continuous subcutaneous infusion. After four weeks of Serp-1 treatment, the effect of Serp-1 was determined by morphometric and immunohistochemical analysis of the resultant plaques.

Methods

Animals
Male ApoE$^{-/-}$ mice (12-14 weeks old) were obtained from TNO-PG (Leiden, The Netherlands). All animal work was approved by the regulatory authority of Leiden and performed in compliance with the Dutch government guidelines. Western type diet and water were provided ad libitum.

Collar Placement and Serp-1 Administration
To determine the effect of Serp-1 on *de novo* atherosclerotic lesion formation, two groups of male ApoE$^{-/-}$ mice (control group: n=8, Serp-1 group: n=9) were fed a Western type diet two weeks before surgery and throughout the experiment. Carotid atherosclerotic lesions were induced by perivascular collar placement as described by von der Thüsen *et al*.[28]. Mice were anaesthetized by subcutaneous injection of ketamine (60 mg/kg, Eurovet Animal Health, Bladel, The Netherlands), fentanyl citrate and fluanisone (1.26 mg/kg and 2 mg/kg respectively, Janssen Animal Health, Saunderton, UK). Sterile osmotic pumps (Alzet, type 2004, Durect Corporation, Cupertino, USA) containing 0.2 µmol/L endotoxin-free Serp-1 in 0.9% saline (2.0 µg/kg/day)[24] were placed subcutaneously using isoflurane anaesthesia one week after collar placement. Two pumps were filled with ^{125}I-Serp-1 (Iodogen method, 0.2 pmol/L, 0.34 cpm/ng) in order to measure plasma levels.
To determine the effect of Serp-1 on advanced atherosclerotic lesions, the administration of Serp-1 (2.0 µg/kg/day) was started in 13 male ApoE$^{-/-}$ (compared to 14 control mice) five weeks after collar placement. Identical osmotic minipumps were used and Serp-1 treatment endured for four weeks. Control mice received osmotic pumps containing PBS. During treatment, plasma total cholesterol levels were measured spectrophotometrically using enzymatic procedures (Roche Diagnostics, Almere, The Netherlands). Triglyceride levels were quantified using a commercially available kit (Roche). In both assays, Precipath standardized serum (Boehringer Mannheim, Mannheim, Germany) was used as an internal standard.

Serum Levels of Serp-1
Radioactivity in plasma, obtained from mice receiving ^{125}I-Serp-1, was measured weekly to quantify plasma concentrations of Serp-1. To determine degradation of Serp-1, 50 µL of plasma containing ^{125}I-Serp-1 was loaded onto a Superdex 75 column in a SMART gel filtration system (Pharmacia, Uppsala, Sweden) and radioactivity in a total of 25 fractions was quantified.

Tissue Harvesting
Animals were anaesthetized after 4 weeks of Serp-1 administration. *In situ* perfusion and tissue embedding occurred as described in von der Thüsen *et al*.[28]. Transverse 5 µm cryosections were prepared on a Leica CM 3050S Cryostat (Leica Instruments, Nassloch, Germany) in a proximal direction for histology and immunohistochemical analysis.

Histology and Immunohistochemistry
Cryosections were stained with hematoxylin (Sigma Diagnostics, Zwijndrecht, The Netherlands) and eosin (Merck Diagnostica, Darmstadt, Germany). Sections were immunohistochemically stained for the presence of macrophages using a rat monoclonal MOMA-2 antibody, dilution 1:50 (a gift from Dr. G. Kraal, VU, Amsterdam, The Netherlands). Rabbit-anti-Rat-biotin (1:300, Sigma Diagnostics) was used as a secondary antibody and ABC-horse radish peroxidase (1:100) was used for visualization. To visualize vSMCs, cryosections were stained for α-smooth muscle actin (ASMA) using an ASMA-fluorescein-isothiocyanate (FITC) conjugated antibody (1:3000, Sigma Diagnostics). Anti-FITC-horse radish peroxidase (1:300) was used as a secondary antibody.
The sections were incubated with primary and secondary antibody for 2 hours at room temperature and stained using 3,3'-diamino-benzidine (Sigma Diagnostics) as enzyme substrate. Sections were stained for collagen, using Picrosirius Red (Direct red 80) and for elastin, using an Accustain elastin staining kit (both Sigma Diagnostics).

Morphometry
Hematoxylin-eosin stained sections of the common carotid arteries were used for morphometric analysis. Each vessel was assessed approx. 0.5 mm proximal to the collar and the site of maximal stenosis was used for morphometric assessment. The images were digitized and analyzed as previously described[28].

Cell Culture
VSMCs were obtained from thoracic aortas from male C57Bl/6 mice using the collagenase digestion method[29]. Cells were cultured in a humidified atmosphere (5% CO_2) at 37°C in DMEM containing 10% Newborn Calf Serum (NCS), 2 mmol/L L-glutamine, 100 U/mL penicillin and 100 µg/mL streptomycin (all from BioWhittaker Europe, Verviers, Belgium).
The murine macrophage cell line RAW 264.7 was cultured in DMEM containing 10% Fetal Bovine Serum (FBS), 2 mmol/L L-glutamine, 100 U/mL penicillin and 100 µg/mL streptomycin in a humidified atmosphere (5% CO_2) and at 37ºC.

Proliferation Assay
VSMCs or RAW cells were detached by short incubation with trypsin-EDTA (BioWhittaker) and seeded at a density of $3.0*10^4$ (vSMCs) or $1.0*10^4$ (RAW)

cells per well. The cells were allowed to attach and serum starved in DMEM containing 1% calf serum for 24 hours to synchronize the cell cycle. The cells were then incubated for 72 hours with medium containing 20 pmol/L of Serp-1 or control medium and medium +/- Serp-1 was refreshed daily. After incubation, 0.5 µCi [^{3}H]thymidine (Amersham, Uppsala, Sweden) per well was added and the cells were incubated at 37°C for 5 hours. [^{3}H]Thymidine incorporation was quantified in a liquid scintillation analyzer (Packard 1500 Tricarb, USA). To verify the validity of the [^{3}H]thymidine incorporation data, also the absolute number of vSMCs and RAW cells was counted using FACS analysis (FACScalibur, BD Biosciences) after 72 hours of exposure to Serp-1 or control medium, starting with 10^5 cells/well.

Migration Assay
VSMCs were serum starved for 24 hours in serum containing 1% NCS prior to the experiment. Cells were detached using trypsin-EDTA and $3.4*10^4$ cells were seeded into Transwell® plates (12 µm filter pores, 12 mm diameter, Costar, Schiphol-Rijk, The Netherlands). On the basolateral side of the Transwell® chamber, medium containing 10% NCS (negative control) or medium containing 10% NCS with 20 pmol/L Serp-1 was added. The chemotactic peptide n-formyl-Methionine-Leucine-Phenylalanine (fMLP, Sigma) was used as a positive control (1 nmol/L). After 4 hours of incubation at 37°C and 5%CO_2, vSMCs were fixed and stained with Mayer´s Hematoxilin. The number of cells that has migrated to the basolateral side of the chamber was scored manually.

Apoptosis Assay
VSMCs and RAW 264.7 were seeded at a density of 10^5 cells/cm^2 and allowed to attach for 24 hours. The cells were exposed to 20 pmol/L of Serp-1 in medium for 24 hours after which DNA of the cells was stained with propidium iodide (Sigma). RNase H (Boehringer Mannheim) was added to avoid RNA contamination in the measurements. DNA fragmentation was measured using FACS analysis (FACScalibur, BD Biosciences).

Statistical Analysis
Values are expressed as mean ± SEM. A 2-tailed Student's t-test was used to compare individual groups of animals. A level of $P<0.05$ was considered significant.

Results

Since the serum half-life of ^{125}I-Serp-1 after intravenous injection into mice was 3.2 minutes, we chose to administer Serp-1 subcutaneously by continuous infusion through osmotic minipumps (infusion rate 0.25 µL/hr/day for 4 weeks, 2.0 µg/kg/day).
Serp-1 infusion did not affect body weight, plasma total cholesterol and triglyceride levels of the Western type diet fed ApoE$^{-/-}$ mice (data not shown). After subcutaneous infusion of Serp-1 by means of the osmotic minipumps, Serp-1 plasma concentration was 14 ± 3 pmol/L (Figure 1A) throughout the duration of the treatment. As a measure of the stability of Serp-1 in plasma, plasma of the ^{125}I-Serp-1 treated mice was analyzed using gel filtration (SMART system, Pharmacia Biotech). The radioactivity profile of each plasma sample essentially coincided with that of intact Serp-1 (Figure 1B), substantiating the integrity of the infused Serp-1. Only in the plasma sampled at week 4, some residual radioactivity was recovered at higher elution volumes, which may point to minor degradation of Serp-1 at that time point.

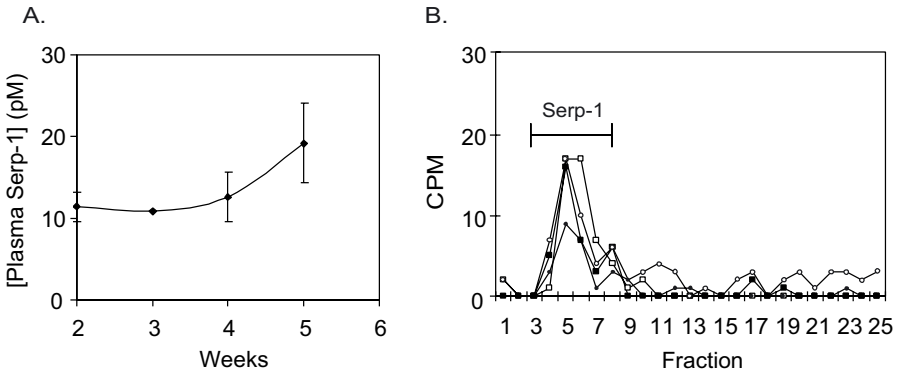

Figure 1. (A) Plasma levels of Serp-1 after continuous subcutaneous infusion of ^{125}I-Serp-1 via an osmotic minipump into ApoE$^{-/-}$ mice during 4 weeks of treatment. (B) Gel filtration analysis of plasma samples obtained from ^{125}I-Serp-1 infused ApoE$^{-/-}$ mice at 2 (□), 3 (■), 4 (○) and 5 (●) weeks after implantation of the osmotic minipumps. The bar indicates the fractions in which intact Serp-1 elutes.

Plaque Size: De Novo Atherogenesis
Plaque size and cell numbers were measured to determine the effect of Serp-1 on *de novo* atherogenesis. Morphometric analysis of lesions proximal to the collar showed that the plaque sizes of Serp-1 treated mice were significantly lower (67.7%) than that of control mice (18 ± 5*10^3 µm^2 versus 57 ± 12*10^3 µm^2 respectively; P=0.007, Figure 2A). Also, the intima/lumen ratio of Serp-1 treated mice was significantly reduced as compared to the control mice (-44%; 0.29 ± 0.06 versus 0.66 ± 0.11, Table 1). Total vessel areas of the carotid artery at the site of maximal stenosis were 79 ± 9*10^3 µm^2 in control animals versus 61 ± 5*10^3 µm^2 on Serp-1 treated mice (P=NS).

Table 1. Effect of Serp-1 on *de novo* atherogenesis: time schedule and morphometric analysis of atherosclerotic carotid artery lesions from control (n=8) and Serp-1 (n=9) treated ApoE$^{-/-}$ mice (mean ± SEM).

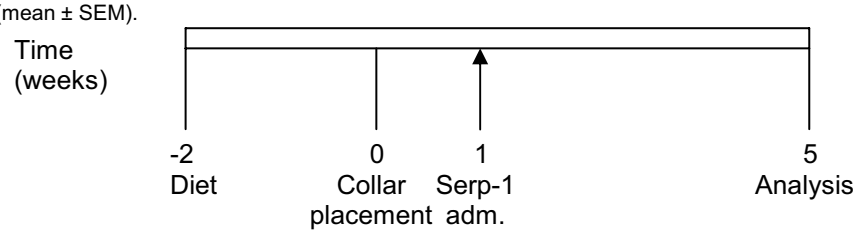

	Control	Serp-1	P-value
Plaque Size (*10^3 µm^2)	57 ± 12	18 ± 5	0.007**
Media Size (*10^3 µm^2)	52 ± 9	30 ± 8	0.08
Intima/Media ratio	1.3 ± 0.4	0.7 ± 0.2	0.19
Intima/Lumen ratio	0.7 ± 0.1	0.3 ± 0.1	0.009**
Lumen Size (*10^3 µm^2)	23 ± 6	43 ± 5	0.017*

Plaque Size: Advanced Atherosclerosis

Analysis of the carotid arteries of the ApoE$^{-/-}$ mice with pre-existing lesions showed a 30% decrease in lesion size after Serp-1 treatment (P=0.058, Figure 2D, Table 2). The lesion size of these Serp-1 treated animals showed a 10% increase in further plaque growth compared to the control mice after 5 weeks of lesion development (P=0.7). Also, the lumen size was significantly increased in treated animals (P=0.028, Figure 2E). Total vessel areas at the site of maximal stenosis was 95 ± 11*10^3 µm^2 in control animals versus 80 ± 7*10^3 µm^2 on Serp-1 treated mice (P=NS).

Table 2. Effect of Serp-1 on pre-existing atherosclerotic lesions: time schedule and morphometric analysis of lesions (control: n=12, Serp-1: n=13, mean ± SEM).

	Control	Serp-1	P-value
Plaque Size (*10^3 µm^2)	89 ± 12	63 ± 7	0.058
Media Size (*10^3 µm^2)	44 ± 10	40 ± 8	0.73
Intima/Media ratio	2.6 ± 0.5	1.9 ± 0.3	0.16
Intima/Lumen ratio	0.9 ± 0.1	0.3 ± 0.1	0.063
Lumen Size (*10^3 µm^2)	6 ± 2	17 ± 4	0.028*

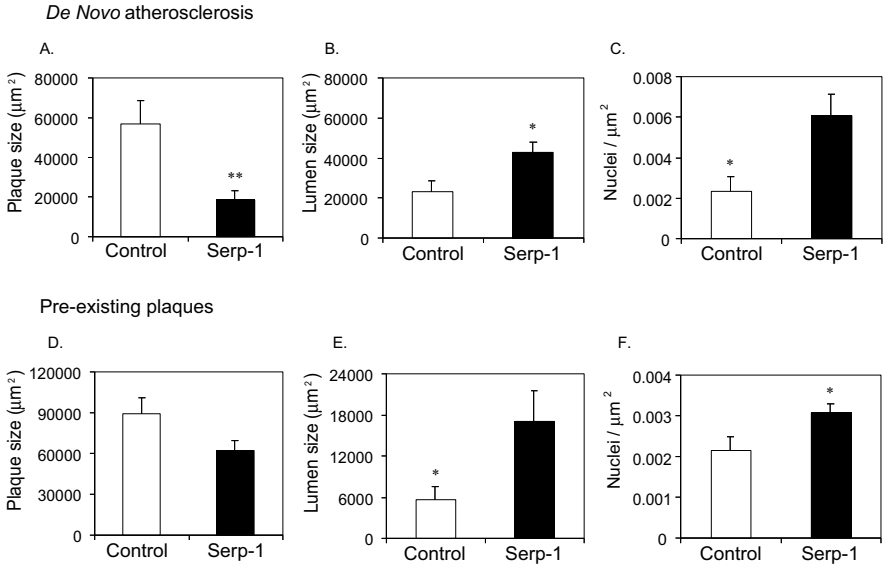

Figure 2. Plaque size analysis (A+D), lumen size (B+E), and cellularity (C+F) of cross-sections of carotid artery specimens obtained from control and Serp-1 treated ApoE$^{-/-}$ mice (*de novo* atherosclerosis: A, B and C, advanced lesions: D, E and F). Error bars represent SEM. (A) Plaque sizes of Serp-1 treated mice compared to that of control mice are significantly reduced (P=0.007**). (B) An increase in lumen size was found in Serp-1 treated ApoE$^{-/-}$ mice (P=0.017*). (C) Cellularity of lesions control mice and Serp-1 treated mice. A significant increase of cellularity was found in the Serp-1 treated group (P=0.014*). (D) Plaque size of Serp-1 treated mice after 5 weeks of collar (P=0.058). (E) Lumen size of Serp-1 treated plaques were found to be increased compared to the controls (P=0.028*). (F) Serp-1 treated lesions also display a significant increase in cellularity (P=0.034*).

Plaque Morphology: De Novo Atherogenesis

A detailed analysis of the plaque morphology revealed striking differences in lesion composition between Serp-1 treated and control mice. When mice were treated with Serp-1 one week after collar placement (*de novo* atherogenesis), lesions were found to differ markedly from that of control mice in terms of core cellularity ($6.0 \pm 1.0*10^3$ cells/mm^2 versus $2.0 \pm 0.7*10^3$ cells/mm^2; P = 0.014, Figure 2C). To address the actual cell type responsible for the increased cellularity, lesions were stained for the presence of macrophages (MOMA-2) and differentiated SMCs (ASMA).

Immunostaining showed a significant decrease in MOMA-2 stained lesion area of Serp-1 treated mice. The area stained for MOMA-2 as a percentage of the total lesion size was 39 ± 5% in control mice versus 20 ± 3% in Serp-1 treated mice (-50%, P=0.004, Figures 3A, B and C). Lesions of Serp-1 treated mice tended to be enriched in α-smooth muscle-actin, calculated as a percentage of total plaque area (control: 9 ± 2%, Serp-1: 14 ± 5%, Figures 3D, E and F). The contribution of extracellular matrix to the plaque structure was determined by measuring collagen content of the lesions using a

Picrosirius Red staining, which showed a significant increase in collagen in Serp-1 treated lesions (38 ± 9% compared to 12 ± 3% in control lesions, P=0.012, Figures 3G, H and I).

Plaque Morphology: Advanced Atherosclerosis

The plaque cellularity of the pre-existing lesions treated with Serp-1 was found to be increased in Serp-1 treated mice compared to control mice (3.1 ± $0.2*10^3$ and 2.1 ± $0.4*10^3$ cells/mm^2 respectively, P=0.034, Figure 2F). Immunostaining in these Serp-1 treated lesions showed a 3-fold increase in α-smooth muscle-actin staining as percentage of the total plaque area compared to the controls (15 ± 5% and 5 ± 1% respectively, P=0.017, Figures 4D, E and F). These data show that in control animals the amount of α-actin is diminishing in time, whereas this is not observed in Serp-1 treated animals. In the lesions the macrophage-specific MOMA-2 staining showed no differences between control and Serp-1 treated mice (15 ± 2% vs. 15 ± 2%, Figures 4A, B and C). In control animals the macrophage content of the plaques decreases in time from 38% to only 15% of the total plaque area. In Serp-1 treated mice, the macrophage content is not increasing during lesion development at the expense of necrotic core formation. The Serp-1 treated plaques contained a significantly higher amount of collagen: 49 ± 3% compared to 27 ± 4% in control plaques (P=0.001, Figures 4G, H and I). In control lesions, collagen was mainly present in the cap of the plaque, in contrast with the treated plaques, which show collagen staining in both cap and core. Elastin staining of the cryosections showed no difference in lesional elastin content (4.8 ± 1.1% in the control group vs. 4.7 ± 0.9% in the Serp-1 treated group). Likewise, fibrin staining did not reveal any differences in fibrin content of the control lesions (19 ± 6%) versus Serp-1 treated arteries (16 ± 4%, P=0.7).

In Vitro Studies

In order to explain the hypercellularity of the Serp-1 treated lesions, *in vitro* experiments were performed using vSMCs. Proliferation studies with vSMCs showed an increased [^{3}H]thymidine incorporation in vSMC exposed to 20 pmol/L of Serp-1, corresponding with the plasma concentration used in the *in vivo* experiments, compared to control vSMCs (170% ± 12% vs. 100% ± 20% in control cells, P=0.003, Figure 5A). FACS analysis confirmed that Serp-1 incubation (20 pmol/L) led to an increase in vSMC count (62,485 ± 5,023 cells compared to 47,031 ± 3,574 control cells, P=0.04, figure 5B). Serp-1 incubation also resulted in a small but significant increase (35%) in [^{3}H]thymidine incorporation ($P<0.05$) in RAW 264.7 cells. However, the absolute number of RAW cells was not significantly altered after Serp-1 exposure (40,626 ± 4,212 vs. 53,311 ± 4,750 cells for the control). This indicates that the increased incorporation of [^{3}H]thymidine was due to increased expansion rather than to increased proliferation of the RAW cells.

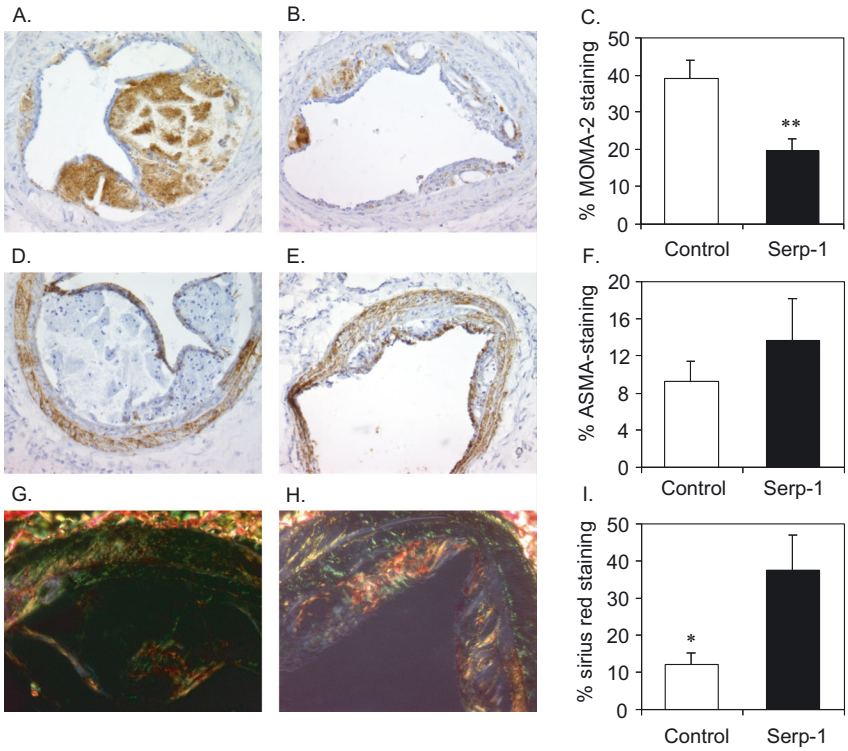

Figure 3. Immunohistochemical analysis of Serp-1 treated and control plaques on the effect of Serp-1 on *de novo* atherogenesis. MOMA-2 staining (100x, A+B), ASMA staining (100x, D+E), and Picrosirius Red staining (200x, G+H) of control (A+D+G) and Serp-1-treated (B+E+H) lesions. Content was calculated as % of staining area relative to the total plaque size. A significant decrease in MOMA-2 positive macrophage content was observed in the Serp-1 treated mice (C; P=0.004**). (F) Amount of α-smooth muscle-actin staining. No significant difference between the relative area stained for vSMCs between control and Serp-1 was observed. (I) Picrosirius red stained collagen was significantly increased in the Serp-1 treated mice (P=0.012*).

In analogy to PAI-1, Serp-1 may promote vSMC migration. Indeed, our vSMC migration assay data clearly demonstrate a highly significant increase of vSMC migration across the filter, when cells were exposed to 20 pmol/L of Serp-1 on the basolateral side of the Transwell® chamber. Incubation of vSMCs with Serp-1 resulted in a transmigration of 386 ± 17 cells per microscopic field compared to 63 ± 9 cells per field in control vSMCs (P=0.003, Figure 5C). Incubation of vSMCs with the chemotactic peptide fMPL, which was used as a positive control, resulted in a transmigration of 290 ± 10 cells per microscopic field.

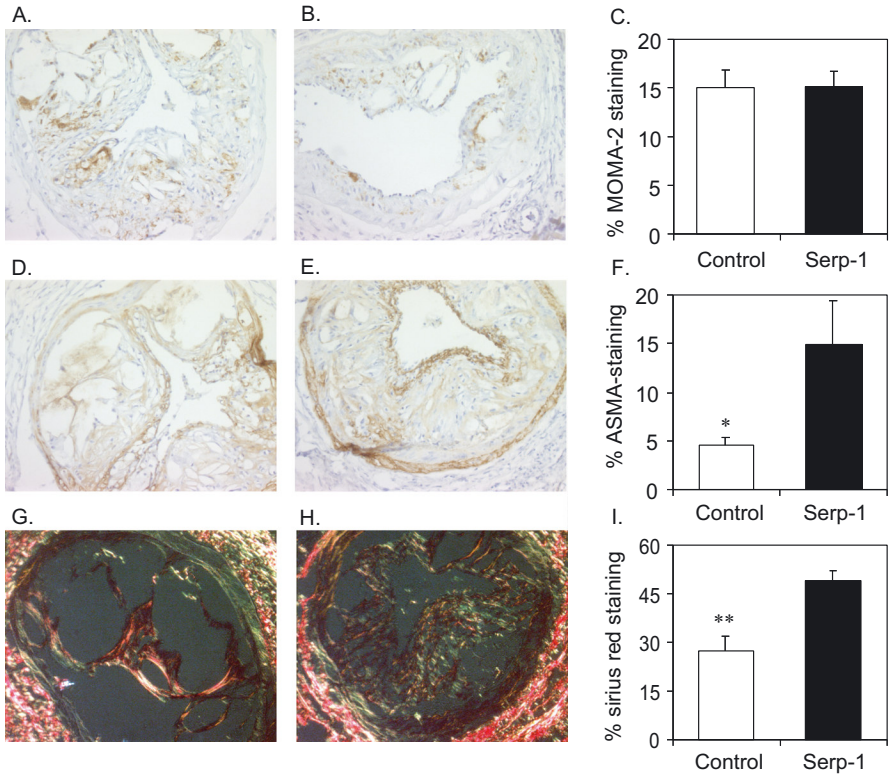

Figure 4. Immunohistochemical analysis of Serp-1-treated and control plaques on the effect of Serp-1 on advanced lesions. MOMA-2 staining (200x, A+B), ASMA staining (200x, D+E), and Picrosirius Red staining (200x, G+H) of control (A+D+G) and Serp-1-treated (B+E+H) lesions. Content was calculated as % of staining area relative to the total plaque size. (C) Extent of MOMA-2 staining. No significant difference between the relative area stained for macrophages between control and Serp-1 was observed. (F) Amount of ASMA staining: α-actin content was found to be significantly increased in Serp-1 treated mice (P=0.017*). (I) A significant increase in collagen in Serp-1 treated mice was measured (P=0.001**).

In the apoptosis assay, incubation of vSMCs and RAW 264.7 murine macrophage cells with 20 pmol/L of Serp-1 did not lead to DNA fragmentation, indicating that Serp-1 did not induce apoptosis in either cell type (data not shown) at concentrations used in the *in vivo* situation.

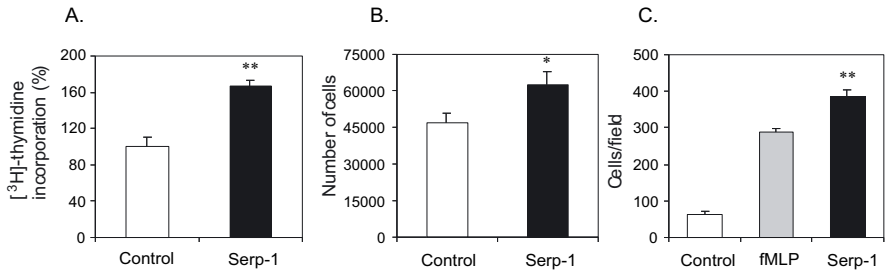

Figure 5. *In vitro* studies performed with vSMCs. (A) Proliferation assay of vSMC exposed to 20 pmol/L of Serp-1, [^{3}H]thymidine incorporation was used to measure proliferation. Exposed to Serp-1, vSMC display a significantly higher tendency to proliferate (P=0.003**). (B) The amount of vSMC after exposure to 20 pmol/L of Serp-1 was significantly increased compared to the number of control cells (P=0.04*). Thus, increase in proliferation shown by [^{3}H]thymidine incorporation was mainly due to an increased number of cells rather than expansion of the vSMCs. (C) Migration assay of vSMCs exposed to 20 pmol/L of Serp-1 at the basolateral side of a Transwell® filter. A significant higher number of vSMCs migrated in the presence of Serp-1 compared to the negative control, P=0.003**. Serp-1 appeared to be an even more potent chemoattractant for vSMCs than the established chemotactic peptide fMPL, (positive control: 1 nmol/L).

Discussion

In this study, the effect of the myxoma virus derived serine protease inhibitor Serp-1 was investigated on *de novo* atherosclerosis and on advanced atherosclerotic lesions in ApoE$^{-/-}$ mice equipped with a perivascular collar to induce carotid artery lesions[28]. Serp-1 treatment led to a striking reduction in *de novo* lesion formation, while Serp-1 did not affect plasma total cholesterol and triglyceride levels as well as the total body weight of the animals or promote outward remodelling of the carotid artery. Plasma levels of Serp-1 after subcutaneous infusion remained constant during treatment at approximately 13.5 pmol/L. These low picomolar Serp-1 levels have been reported to suffice for effective serine protease inhibition and for blocking the host's immune response to myxoma infection[20,21]. Further gel filtration analysis revealed that Serp-1 was not degraded during the timeframe of the experiment. Blood cell levels did not differ between control and Serp-1 treatment groups, suggesting that Serp-1 did not act atheroprotective by inducing a systemic anti-inflammatory response.

Interestingly, a 3-fold increase in plaque cellularity was observed in the Serp-1 treated mice. The nature of the cells responsible for the hypercellularity of Serp-1 lesions remains to be elucidated. The plaque macrophage content was shown to be reduced by 50%. Moreover, we did not observe a significant difference in ASMA positive vSMC content between control and treated mice. Conceivably, the vascular wall may be enriched in vSMCs that are redifferentiated towards an ASMA negative phenotype, previously reported to be present in atherosclerotic lesions[30,31]. This is in keeping with the fact that plaque collagen content was found to be increased by Serp-1 treatment.

Furthermore, our *in vitro* studies showed that vSMCs proliferate and display an enhanced tendency to migrate when exposed to Serp-1 at concentrations used in *in vivo* experiment, indicating that the hypercellularity of the lesions may indeed be explained by an increased vSMC content.
In line with the anti-inflammatory effect of Serp-1 as proposed by Macen *et al.*[20], the observed 50.4% reduction in macrophage content of *de novo* formed lesions suggests that Serp-1 acts partly by impairing monocyte recruitment when administered while the atherosclerotic plaque is formed. The murine macrophage cell line RAW 264.7 showed no increase in apoptosis of these cells upon exposure to Serp-1, indicating that the decrease in macrophage content in the lesions cannot be explained by apoptosis of macrophages in the plaque, but may be caused by an impaired monocyte influx. A similar inhibitory effect of Serp-1 on monocyte infiltration was reported by Lucas *et al.*[24].
To elucidate the effect of Serp-1 on lesion progression and development, the effect of Serp-1 on advanced lesions was determined by initiating Serp-1 treatment 5 weeks after collar placement. Plaque size and morphology analysis showed an almost 30% decrease in plaque size and a significant 3-fold increase in lumen size. Importantly, total vessel area was not affected by Serp-1 treatment. This indicates that Serp-1 did not promote outward remodelling of the arteries and that the risk of aneurysm formation after Serp-1 treatment is minor. The plaque size of these Serp-1 treated arteries ($57*10^3$ μm^2) is similar to the plaque size of control arteries ($63*10^3$ μm^2) in the study on *de novo* atherogenesis, suggesting that plaque progression is almost completely blunted by Serp-1 administration. Importantly, a significant increase in cellularity of the plaque was again observed in Serp-1 treated mice, which in this study can be explained by an increase in amount of α-actin positive vSMCs. The lesional vSMC content in control animals decreased in time, suggesting apoptosis of vSMCs in the cap[32], which may be inhibited by Serp-1.
The Serp-1 treated lesions were found to be was enriched in collagen, which was not only present in the cap, but also in the core, as was also observed in the study on *de novo* atherogenesis. Quantitative gene expression analysis of vSMC after exposure to 20 pmol/L of Serp-1 did not demonstrate an effect on pro-collagen-I mRNA levels (data not shown), pointing to an effect of Serp-1 on collagen degradation in the lesion rather than to an increase in production of collagen. Plasmin, activated by uPA and tPA, is a potent activator of collagenase (MMP-1), stromelysin (MMP-3) and gelatinases (MMP-2 and -9), which are matrix-metalloproteinases (MMPs)[33], commonly present in atherosclerotic lesions. Conceivably, an impaired activation of MMPs via inhibition of uPA by Serp-1 can lead to increased collagen content in the lesions. Therefore, Serp-1 may promote a stable plaque phenotype by increasing collagen and α-actin positive smooth muscle cell content. Macrophage-specific MOMA-2 staining did not reveal differences in macrophage content between the groups of mice. It should be realized, however, that macrophage infiltration is a process mainly occurring in the

early stage of atherogenesis rather than in later stages of lesion development[1], thus proceeding prior to administration of Serp-1. We did show a decrease in macrophage content of the lesions in control mice in time from 40% to 15% at the expense of enhanced necrotic core formation, which was not observed in Serp-1 treated animals.
The activity profile of Serp-1 considerably overlaps with that of PAI-1 in that both are potent inhibitors of uPA, tPA, and plasmin. Comparison of the effects of Serp-1 to that of PAI-1 may thus hold a key to elucidation of the actual mechanism by which Serp-1 exerts its atheroprotective effect. Unfortunately, conflicting data on PAI-1[2,12,13] emphasize that the effects of modulation of serine protease activity are intricately dependent on the local protease milieu and the disease progression and leave unanswered to what extent anti-inflammatory effects of Serp-1 may contribute to its beneficial effect as well. Other studies on the role of tPA and uPA in atherogenesis have shown that overexpression of uPA in carotid arteries in rabbits results in an acceleration of plaque growth, although no difference in plaque morphology was observed[34]. Carmeliet *et al*.[35] have shown that in $uPA^{-/-}$ mice neointima formation after electric injury is reduced. However, in $uPA^{-/-}$ mice, vSMC migration was found to be reduced, suggesting that additional effects are involved in the Serp-1 effect as well. Just recently, data by Dai *et al.* [36] indicate that Serp-1 acts through an uPA receptor dependent mechanism, as atherosclerosis after allograft transplantation of $uPAR^{-/-}$ aortas to $uPAR^{+/+}$ animals was not affected by Serp-1 treatment.
In conclusion, the viral glycoprotein Serp-1 inhibited *de novo* carotid artery plaque growth in $ApoE^{-/-}$ mice by a significant 68%. This inhibition was mainly caused by a striking reduction in macrophage infiltration. On advanced lesions, Serp-1 inhibited plaque growth with almost 30%. Serp-1 was found to induce hypercellularity and increased the collagen content of the lesion core suggestive of improved plaque stability. The above results thus indicate that Serp-1 or serpins as a general class of anti-inflammatory proteases constitute an attractive lead in anti-atherosclerotic therapy.

References

1. Lusis AJ. Atherosclerosis. *Nature*. 2000;407:233-241.
2. Carmeliet P, Moons L, Dewerchin M, Mackman N, Luther T, Breier G, Ploplis V, Muller M, Nagy A, Plow E, Gerard R, Edgington T, Risau W, Collen D. Insights in vessel development and vascular disorders using targeted inactivation and transfer of vascular endothelial growth factor, the tissue factor receptor, and the plasminogen system. *Ann N Y Acad Sci*. 1997;811:191-206.
3. Moons AH, Levi M, Peters RJ. Tissue factor and coronary artery disease. *Cardiovasc Res*. 2002;53:313-325.
4. Eitzman DT, Westrick RJ, Xu Z, Tyson J, Ginsburg D. Plasminogen activator inhibitor-1 deficiency protects against atherosclerosis progression in the mouse carotid artery. *Blood*. 2000;96:4212-4215.
5. Torzewski J, Bowyer DE, Waltenberger J, Fitzsimmons C. Processes in atherogenesis: complement activation. *Atherosclerosis*. 1997;132:131-138.
6. Niculescu F, Rus H. Complement activation and atherosclerosis. *Mol Immunol*. 1999;36:949-955.
7. Naito M, Hayashi T, Kuzuya M, Funaki C, Asai K, Kuzuya F. Effects of fibrinogen and fibrin on the migration of vascular smooth muscle cells in vitro. *Atherosclerosis*. 1990;83:9-14.

8. Torzewski J, Oldroyd R, Lachmann P, Fitzsimmons C, Proudfoot D, Bowyer D. Complement-induced release of monocyte chemotactic protein-1 from human smooth muscle cells. A possible initiating event in atherosclerotic lesion formation. *Arterioscler Thromb Vasc Biol*. 1996;16:673-677.
9. Goldsack NR, Chambers RC, Dabbagh K, Laurent GJ. Thrombin. *Int J Biochem Cell Biol*. 1998;30:641-646.
10. Kusch A, Gulba DC. Significance of the uPA/uPAR system for development of arteriosclerosis and restenosis. *Z Kardiol*. 2001;90:307-318.
11. Ye S, Goldsmith EJ. Serpins and other covalent protease inhibitors. *Curr Opin Struct Biol*. 2001;11:740-745.
12. Sjoland H, Eitzman DT, Gordon D, Westrick R, Nabel EG, Ginsburg D. Atherosclerosis progression in LDL receptor-deficient and apolipoprotein E-deficient mice is independent of genetic alterations in plasminogen activator inhibitor-1. *Arterioscler Thromb Vasc Biol*. 2000;20:846-852.
13. Luttun A, Lupu F, Storkebaum E, Hoylaerts MF, Moons L, Crawley J, Bono F, Poole AR, Tipping P, Herbert JM, Collen D, Carmeliet P. Lack of plasminogen activator inhibitor-1 promotes growth and abnormal matrix remodeling of advanced atherosclerotic plaques in apolipoprotein E-deficient mice. *Arterioscler Thromb Vasc Biol*. 2002;22:499-505.
14. DeYoung MB, Tom C, Dichek DA. Plasminogen activator inhibitor type 1 increases neointima formation in balloon-injured rat carotid arteries. *Circulation*. 2001;104:1972-1977.
15. Ploplis VA, Castellino FJ. Attenuation of neointima formation following arterial injury in PAI-1 deficient mice. *Ann N Y Acad Sci*. 2001;936:466-468.
16. Zhu Y, Farrehi PM, Fay WP. Plasminogen activator inhibitor type 1 enhances neointima formation after oxidative vascular injury in atherosclerosis-prone mice. *Circulation*. 2001;103:3105-3110.
17. Ploplis VA, Cornelissen I, Sandoval-Cooper MJ, Weeks L, Noria FA, Castellino FJ. Remodeling of the vessel wall after copper-induced injury is highly attenuated in mice with a total deficiency of plasminogen activator inhibitor-1. *Am J Pathol*. 2001;158:107-117.
18. Upton C, Macen JL, Wishart DS, McFadden G. Myxoma virus and malignant rabbit fibroma virus encode a serpin-like protein important for virus virulence. *Virology*. 1990;179:618-631.
19. Upton C, Macen JL, Schreiber M, McFadden G. Myxoma virus expresses a secreted protein with homology to the tumor necrosis factor receptor gene family that contributes to viral virulence. *Virology*. 1991;184:370-382.
20. Macen JL, Upton C, Nation N, McFadden G. SERP1, a serine proteinase inhibitor encoded by myxoma virus, is a secreted glycoprotein that interferes with inflammation. *Virology*. 1993;195:348-363.
21. Nash P, Lucas A, McFadden G. SERP-1, a poxvirus-encoded serpin, is expressed as a secreted glycoprotein that inhibits the inflammatory response to myxoma virus infection. *Adv Exp Med Biol*. 1997;425:195-205.
22. Lomas DA, Evans DL, Upton C, McFadden G, Carrell RW. Inhibition of plasmin, urokinase, tissue plasminogen activator, and C1S by a myxoma virus serine proteinase inhibitor. *J Biol Chem*. 1993;268:516-521.
23. Nash P, Whitty A, Handwerker J, Macen J, McFadden G. Inhibitory specificity of the anti-inflammatory myxoma virus serpin, SERP-1. *J Biol Chem*. 1998;273:20982-20991.
24. Lucas A, Liu L, Macen J, Nash P, Dai E, Stewart M, Graham K, Etches W, Boshkov L, Nation PN, Humen D, Hobman ML, McFadden G. Virus-encoded serine proteinase inhibitor SERP-1 inhibits atherosclerotic plaque development after balloon angioplasty. *Circulation*. 1996;94:2890-2900.
25. Hausen B, Boeke K, Berry GJ, Morris RE. Viral serine proteinase inhibitor (SERP-1) effectively decreases the incidence of graft vasculopathy in heterotopic heart allografts. *Transplantation*. 2001;72:364-368.
26. Miller LW, Dai E, Nash P, Liu L, Icton C, Klironomos D, Fan L, Nation PN, Zhong R, McFadden G, Lucas A. Inhibition of transplant vasculopathy in a rat aortic allograft model after infusion of anti-inflammatory viral serpin. *Circulation*. 2000;101:1598-1605.
27. Lucas A, Dai EB, Liu LY, Guan HY, Nash P, McFadden G, Miller L. Transplant vasculopathy: Viral anti-inflammatory serpin regulation of atherogenesis. *J Heart Lung Transplantation*. 2000;19:1029-1038.

28. von der Thüsen JH, van Berkel TJC, Biessen EAL. Induction of rapid atherogenesis by perivascular carotid collar placement in apolipoprotein E-deficient and low-density lipoprotein receptor-deficient mice. *Circulation*. 2001;103:1164-1170.
29. Michon IN, Hauer AD, von der Thüsen JH, Molenaar TJM, van Berkel TJC, Biessen EAL, Kuiper J. Targeting of peptides to restenotic vascular smooth muscle cells using phage display in vitro and in vivo. *Biochim Biophys Acta*. 2002;1591:87-97.
30. Babaev VR, Bobryshev YV, Stenina OV, Tararak EM, Gabbiani G. Heterogeneity of smooth muscle cells in atheromatous plaque of human aorta. *Am J Pathol*. 1990;136:1031-1042.
31. Kocher O, Gabbiani G. Cytoskeletal features of normal and atheromatous human arterial smooth muscle cells. *Hum Pathol*. 1986;17:875-880.
32. Bennett MR. Apoptosis in the cardiovascular system. *Heart*. 2002; 87: 480-487.
33. Van den Steen PE, Opdenakker G, Wormald MR, Dwek RA, Rudd PM. Matrix remodelling enzymes, the protease cascade and glycosylation. *Biochim Biophys Acta*. 2001; 1528:61-73.
34. Falkenberg M, Tom C, DeYoung MB, Wen S, Linnemann R, Dichek DA. Increased expression of urokinase during atherosclerotic lesion development causes arterial constriction and lumen loss, and accelerates lesion growth. *PNAS*. 2002;99:10665-10670.
35. Carmeliet P, Moons L, Herbert J-M, Crawley J, Lupu F, Lijnen R, Collen D. Urokinase but not tissue plasminogen activator mediates arterial neointima formation in mice. *Circ Res*. 1997;81:829-839.
36. Dai E, Guan H, Liu L, Little S, McFadden G, Vaziri S, Cao H, Ivanova IA, Bocksch L, Lucas A. Serp-1, a viral anti-inflammatory serpin, regulates cellular serine proteinase and serpin responses to vascular injury. *J Biol Chem*. 2003; 278:18563-72.